



Secrecy Outage Probability of Secondary System for Wireless-Powered Cognitive Radio Networks

Kun Tang¹(✉), Shaowei Liao¹, Md. Zakirul Alam Bhuiyan², and Wei Shi³

¹ School of Electronic and Information Engineering,
South China University of Technology, Guangzhou 510640, China
{tangkun,liaoshaowei}@scut.edu.cn

² Department of Computer and Information Sciences,
Fordham University, New York 10023, USA
mbhuiyan3@fordham.edu

³ School of Information Technology,
Carleton University, Ottawa K1S 5B6, Canada
wei.shi@carleton.ca

Abstract. In this paper, we consider a secrecy wireless-powered cognitive radio network, where an energy harvesting secondary system can share the spectrum of the primary system by assisting its transmission. In particular, we focus on the secure information transmission for the secondary system when an eavesdropper is existed to intercept the secondary user's confidential information. Closed-form analytical expressions of primary outage probability, secondary secrecy outage probability (SOP) and the probability of non-zero secrecy capacity (PNSC) are derived. We also aim to joint design optimal time-switching ratio and power-splitting coefficient for maximizing the secondary secrecy outage probability under primary requirement constraint. To solve this non-convex problem, we prove the biconvexity of optimization problem and then develop a corresponding algorithm to solve that optimization problem. Numerical results show that our proposed transmission scheme can provide greater secure information transmission for secondary system and guarantee the outage performance for primary system.

Keywords: Cognitive radio network · Energy harvesting · Secrecy outage probability · Probability of non-zero secrecy capacity · Biconcave

1 Introduction

With the rapid increase and development of the wireless devices and services, the next generation mobile communication technologies are expected to provide high capacity and low energy consumption transmission services [1]. In the meanwhile, conventional spectrum management strategies also lead that spectrum resources

are under-utilized for most of the time [2]. Therefore, how to effectively achieve these new wireless services and applications under the constraint of limited radio spectrum is becoming an extremely challenge at present. Cognitive radio (CR) technologies have been recognized as a promising method to solve the shortage of spectrum resources, where the secondary users (SUs) can be allowed opportunistically to access the license spectrum for data transmission, which is also known as dynamic spectrum access (DSA) [3].

Energy scarcity is another critical factor affecting the development of wireless communications, especially for sensors and cellular networks, which are generally powered by batteries and it is difficult to be replaced by new ones. To alleviate this, wireless-powered (WP) technology has been paid high attention since the devices can be able to scavenge energy from the surrounding environment into electric energy for future data transmission, such as solar, wind or RF signals [4]. Especially with the concurrent developments in design of antennas and circuits, wireless energy harvesting based on RF signal is more attractive due to its wireless, low cost, and small form factor implementation [5, 6]. Therefore, the combination of cognitive radio networks with energy harvesting can effectively improve both the spectral efficiency and energy efficiency.

Nevertheless, there exists some security issues in WP-based CR networks (WP-CRN) due to the open nature of wireless medium, where several potential eavesdroppers may listen legitimate users' confidential information. To address the secure transmission problems in WP-CRN, physical-layer security has been discussed by [7, 8]. In [7], secure information transmission for the primary system is investigated when the SUs were the potential eavesdroppers. A jointly optimal algorithm to derive the optimized power splitting coefficient and secure beamforming vector were also proposed. The authors of [8] investigated the probability of strictly positive secrecy capacity for a underlay CRN with full-duplex WP secondary system.

In this paper, we study the secure information transmission issue for the secondary system of WP-CRN, where an eavesdropper is existed to intercept the secondary user's confidential information. We derive the closed-form expressions of the primary outage probability, SOP and PNSC of the secondary system. We further aim to maximize the SOP of the secondary system while guaranteeing the outage probability requirement of the primary system. To solve this non-convex problem, the optimization problem is proved as biconcave problem and an effective algorithm is then proposed.

The remainder of this paper is organized as follows. In Sect. 2, the system model is introduced and the spectrum sharing scheme is proposed. Section 3 analyzes the outage probability of the primary system, SOP and PNSC of secondary system. Besides, an algorithm to derive the optimal time-switching ratio and power-splitting coefficient is given in Sect. 4. Simulation and numerical results are presented in Sect. 5. Finally, Sect. 6 concludes this paper.

2 System Model and Transmission Protocol

2.1 System Model

We consider an overlay cognitive radio network with wireless-powered relay (CRN-WPR) as shown in Fig. 1. In the primary system, a PT intends to communicate with a PR by assisting of a ST as relay since large propagation loss and shadowing exists between PT and PR. In the secondary system, the ST delivers its confidential information to desired SR, while a secondary eavesdropper (SE) exists within the transmission range of ST who aims to intercept the ST's confidential information. We assume that PT has a fixed power supply, whereas the ST may have limited battery reserves and needs to have the ability to harvest energy from the received primary radio frequency (RF) signals. All nodes operate at half-duplex mode and are equipped with a single antenna.

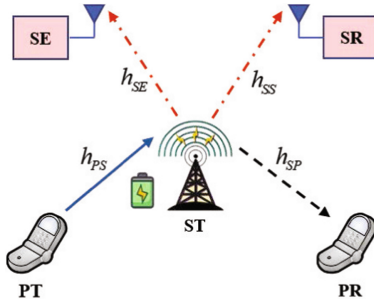


Fig. 1. System model of a CRN-WPR. The blue line denotes the first wireless information and power transfer phase, the black line represents the second information transmission phase, and the red lines denotes the third transmission phase. (Color figure online)

All channels undergo the flat block Rayleigh fading channel, which remains quasi-static in one time slot and changes independently over different time slots. Let h_{PS} , h_{SP} , h_{SS} , and h_{SE} be the channel coefficient between PT and ST, ST and PR, ST and SR, ST and SE, respectively. Thus the channel power gain $|h_A|^2$ with $A = \{PS, SP, SS, SE\}$ is exponentially distributed with zero mean and variance $\lambda_A = d_A^{-\theta}$, where d_A denotes the transmission distance and θ being the path loss exponent. We also assume that the global channel state information (CSI) is available for the ST [7].

2.2 Energy Harvesting and Information Transmission

As shown in Fig. 1, the transfer protocol for a transmission block includes three phases. In the first phase, PT takes a portion of time αT ($0 < \alpha < 1$) to transmit its signal to the relay node ST, the received signal can be expressed by

$$y_{ST} = \sqrt{P_P} h_{PS} x_P + n_{ST}, \quad (1)$$

where P_P denotes the transmission power of primary signal, x_P is the unit-power signal intended for PR, $n_{ST} \sim \mathcal{CN}(0, \delta_{ST})$ represents the additive white Gaussian noise (AWGN) introduced by antenna of relay node ST. Based on power-splitting method, the received signal at the ST can be divided into two streams, one for energy harvesting and the other for relaying information. Thus, the partially received signal for harvested energy is given by

$$\sqrt{\beta}y_{ST} = \sqrt{\beta P_P}h_{PS}x_P + \sqrt{\beta}n_{ST}, \quad (2)$$

where $0 < \beta < 1$ denotes the portion of information splitting for energy harvesting. The amount of harvested energy is then calculated as

$$E(\alpha T) = \alpha T \beta \eta P_P |h_{PS}|^2, \quad (3)$$

where $0 < \eta < 1$ is the energy conversion efficiency. Note that the harvested energy from thermal noise is negligible compared to that of the primary signal. Without loss of generality, we assume $T = 1$ in the followings.

During the second phase $(1 - \alpha)/2$, ST forwards residual primary signal $\sqrt{1 - \beta}y_{ST}$ to PR based on the amplify-and-forward (AF) strategy. The broadcasting information at the ST is $\tilde{x}_P = \omega \sqrt{P_{ST}} (\sqrt{1 - \beta}y_{ST} + n_C)$, where $n_C \sim \mathcal{CN}(0, \delta_C)$ denotes the AWGN introduced by the signal conversion from pass-band to baseband at the ST. ω is the power normalization factor, which is given by

$$\omega = \frac{1}{\sqrt{(1 - \beta) (P_P |h_{PS}|^2 + \delta_{ST}) + \delta_C}}. \quad (4)$$

In practice, the received noise power δ_{ST} is much smaller than the noise δ_{ST} introduced from signal conversion and even lower than the average power of received signal. Moreover, δ_C can be ignored at high signal-noise-ratio (SNR). We thus assume $\delta_{ST} = \delta_C = 0$ to simplify the analysis and the approximated $\tilde{\omega}$ in the rest of this paper is given by

$$\tilde{\omega} = \frac{1}{\sqrt{(1 - \beta) P_P |h_{PS}|^2}}. \quad (5)$$

Therefore, the corresponding received signal at the PR can be expressed as

$$y_{PR} = \sqrt{P_{ST}} \tilde{x}_P h_{SP} + n_{PR} = \sqrt{P_{ST}} \left(\frac{h_{PS} x_P}{\sqrt{|h_{PS}|^2}} + \frac{(1 - \beta) n_{ST} + n_C}{\sqrt{(1 - \beta) P_P |h_{PS}|^2}} \right) h_{SP} + n_{PR}, \quad (6)$$

where $n_{PR} \sim \mathcal{CN}(0, \delta_{PR})$ denotes the AWGN at the PR and $P_{ST} = \frac{\alpha}{1 - \alpha} \beta \eta P_P |h_{PS}|^2$, where the coefficient $\frac{\alpha}{1 - \alpha}$ is following the fact that the half harvested energy is used to transmit information and time duration of each transmission phase is normalized to $\frac{1 - \alpha}{2}$. Thus, the signal-interference-plus-noise ratio (SINR) of PR to derive x_P is given by

$$r_{PR} = \frac{\frac{\alpha}{1 - \alpha} \beta \eta P_P |h_{PS}|^2 |h_{SP}|^2}{\left(\frac{\alpha}{1 - \alpha} \beta \eta \delta_{ST} + \frac{\alpha}{1 - \alpha} \frac{\beta}{1 - \beta} \eta \delta_C \right) |h_{SP}|^2 + \delta_{PR}}. \quad (7)$$

The achievable rate at the PR is then expressed as $C_{PR} = \frac{1-\alpha}{2} \log_2(1 + r_{PR})$.

In the third phase, ST transmits its unit-power signal x_S to SR, while SE can also eavesdrop the x_S because the wireless broadcast nature. The received signals at the ST and SE are respectively given by

$$y_{SR} = \sqrt{P_{ST}} x_S h_{SP} + n_{SR}, \quad y_{SE} = \sqrt{P_{ST}} x_S h_{SE} + n_{SE}, \quad (8)$$

where $n_{SR} \sim \mathcal{CN}(0, \delta_{SR})$ and $n_{SE} \sim \mathcal{CN}(0, \delta_{SE})$ represent the AWGN at the SR and SE, respectively. The corresponding SNR at the SR and SE can be respectively expressed as

$$r_{SR} = \frac{\alpha\beta\eta P_P |h_{PS}|^2 |h_{SR}|^2}{(1-\alpha)\delta_{SR}}, \quad r_{SE} = \frac{\alpha\beta\eta P_P |h_{PS}|^2 |h_{SE}|^2}{(1-\alpha)\delta_{SE}}. \quad (9)$$

For the sake of simplicity, we assume the received noise powers at the SR and SE are the same, i.e., $\delta_{SR} = \delta_{SE} = \delta_0$, in the followings. Accordingly, the achievable data rates at the SR and SE are respectively given by

$$C_{SR} = \frac{1-\alpha}{2} \log_2(1 + r_{SR}), \quad C_{SE} = \frac{1-\alpha}{2} \log_2(1 + r_{SE}). \quad (10)$$

3 Analysis of System Outage Performance

3.1 Outage Probability of the Primary System

An outage event will be occurred if the achievable data rate of the PR is lower than a given target threshold γ_P . Thus, the primary outage probability can be expressed as

$$P_{out}^P = \Pr\{C_{PR} < \gamma_P\}. \quad (11)$$

Based on (7), we have the following proposition.

Proposition 1: Define $l = \alpha\beta\eta P_P / (1-\alpha)$, $m = \frac{\alpha\beta\eta}{1-\alpha} \left(\delta_{ST} + \frac{\delta_C}{1-\beta} \right)$, and $\tilde{\gamma}_P = 2^{2\gamma_P/(1-\alpha)} - 1$. Let $X = |h_{PS}|^2$ and $Y = |h_{SP}|^2$. The primary outage probability in the considering cognitive radio networks is given by

$$P_{out}^P = 1 + Q_1^2 - Q_1 Q_2 - Q_1, \quad (12)$$

where

$$Q_1 = \exp\left(-\frac{\tilde{\gamma}_P m}{l \lambda_{PS}}\right), \quad (13)$$

$$Q_2 = \frac{1}{\lambda_{PS}} \exp\left(-\frac{\tilde{\gamma}_P m}{l \lambda_{PS}}\right) \sqrt{\frac{4\tilde{\gamma}_P \delta_{PR} \lambda_{PS}}{l \lambda_{SP}}} \mathcal{K}_1\left(\sqrt{\frac{4\tilde{\gamma}_P \delta_{PR}}{l \lambda_{PS} \lambda_{SP}}}\right) \quad (14)$$

with $\mathcal{K}_1(\cdot)$ denoting the modified Bessel function of the second kind with the first-order, which is defined in [9].

Proof: The proof is provided in Appendix A.

3.2 Secrecy Outage Performance of the Secondary System

The SOP is defined that the probability of the achievable secrecy rate is smaller than a given threshold C_{th} . Based on the analyses of (9) and (10), the achievable secrecy rate of the secondary system is given by

$$C_S = \left[\frac{1-\alpha}{2} \log_2(1+r_{SR}) - \frac{1-\alpha}{2} \log_2(1+r_{SE}) \right]^+, \quad (15)$$

where $[x]^+$ represents the maximum value between x and 0. Therefore, the SOP of the secondary system is expressed as

$$P_{SOP}^S = \Pr \{C_S < C_{th}\} = \Pr \left\{ \frac{1-\alpha}{2} \log_2(r_{SOP}^S) < C_{th} \right\}, \quad (16)$$

where $r_{SOP}^S = (1+r_{SR})/(1+r_{SE})$.

Proposition 2: Define $\tilde{C}_{th} = 2^{2C_{th}/(1-\alpha)}$ and the SOP of the secondary system is then given by

$$P_{SOP}^S = 1 + T_1^2 - T_1 T_2 - T_1, \quad (17)$$

where

$$T_1 = \frac{\lambda_{SR}}{\lambda_{SR} + \lambda_{SE} \tilde{C}_{th}}, \quad (18)$$

$$T_2 = \frac{1}{\lambda_{SR} + \lambda_{SE} \tilde{C}_{th}} \sqrt{\frac{4\delta_0 (\tilde{C}_{th} - 1) \lambda_{SR}}{l\lambda_{PS}}} \mathcal{K}_1 \left(\sqrt{\frac{4\delta_0 (\tilde{C}_{th} - 1)}{l\lambda_{PS} \lambda_{SR}}} \right). \quad (19)$$

The proof is omitted since the process is similar as the Proposition 1.

The PNSC is defined as the probability of existing a positive secrecy capacity between SR and SE. Based on (16), the PNSC can be written as

$$P_{PNSC}^S = 1 - P_{SOP}^S (C_{th} \leq 0). \quad (20)$$

In this case, we can obtain $0 < \tilde{C}_{th} \leq 1$ when $C_{th} \leq 0$ from equation (16), which means the received SNR at the SR is less than the received SNR at the SE, i.e., $r_{SR} \leq r_{SE}$. Therefore, the PNSC is only related to the channel power gain ratio $|h_{SR}|^2/|h_{SE}|^2$. After some algebraic manipulation, we have

$$P_{PNSC}^S = \frac{\lambda_{SR}}{\lambda_{SR} + \lambda_{SE}}. \quad (21)$$

4 Optimal Time-Switching Ratio and Power-Splitting Coefficient

4.1 Optimization Problem Analysis

Following the above-mentioned analyses of system outage performance, we can obtain that the improved data transfer rate means reducing the SOP and enhancing PNSC of the secondary system. Moreover, optimizing data transfer rate can also increase energy efficiency, which means that a given amount of energy can be utilized to transmit more information. Therefore, in this section, we focus on the design of optimal time-switching ratio and power-splitting coefficient for maximizing the secondary secrecy rate under the primary user's rate, the power time-switching ratio, and power splitting coefficient constraints. Mathematically, the optimal scheme can be represented as the following optimization problem (P1):

$$\begin{aligned} \max_{\alpha, \beta} \quad & C_S = \left[\frac{1-\alpha}{2} \log_2(1+r_{SR}) - \frac{1-\alpha}{2} \log_2(1+r_{SE}) \right]^+ \\ \text{s.t.} \quad & \text{C1: } C_{PR} \geq r_P; \\ & \text{C2: } 0 < \alpha < 1; \\ & \text{C3: } 0 < \beta < 1. \end{aligned} \quad (22)$$

In (24), the value of the objective function should large than zero, which is equivalent to the channel gain between ST and SE should lower than the channel gain between ST and SR, i.e., $|h_{SR}|^2 > |h_{SE}|^2$.

Obviously, the optimization problem (P1) is a non-convex problem, which is difficult to obtain the optimal parameters (α^* , β^*) concurrently. In the followings, we thus first demonstrate that (P1) is actually a biconcave optimization problem, and then propose an algorithm to solve that biconcave problem.

Definition 1: Let $X \subseteq \mathbb{R}^n$ and $Y \subseteq \mathbb{R}^m$ are two independent non-empty and concave sets, and define set $B \subseteq X \times Y$. The x - and y -sections of B are expressed as $B_x := \{y \in Y : (x, y) \in B\}$, $B_y := \{x \in X : (x, y) \in B\}$. If B_x is concave for every $x \in X$ and B_y is concave for every $y \in Y$, the set $B \subseteq X \times Y$ will be a biconcave set on $X \times Y$ [10].

Definition 2: If function $f_x(\cdot) := f(x, \cdot) B_x \rightarrow \mathbb{R}$ is concave function on B_x for each fixed $x \in X$, while function $f_y(\cdot) := f(y, \cdot) B_y \rightarrow \mathbb{R}$ is concave function on B_y for each fixed $y \in Y$, a function $f : B \rightarrow \mathbb{R}$ on a biconcave set $B \subseteq X \times Y$ is named as a biconcave function [10].

Definition 3: If the feasible set B is biconcave on $X \times Y$, while the objective function f is biconcave on B , the corresponding optimization problem $\max \{f(x, y) : (x, y) \in B\}$ is called a biconcave optimization problem.

Theorem 1: Let f denote a real-valued function on $X \times Y$, where $X \subseteq \mathbb{C}^n$ and $Y \subseteq \mathbb{C}^m$ are two independent non-empty and concave sets. If f is biconcave on $X \times Y$, then its level sets $L_C := \{(x, y) \in X \times Y : f(x, y) \leq c\}$ are biconcave for every $c \in \mathbb{C}$.

Based on above-mentioned results, let $\mathcal{G}(\alpha, \beta)$ and $\mathcal{H}(\alpha, \beta)$ represent objective function and constraint functions C1 in (22), respectively. The feasible sets of α and β are denoted as \mathbb{E} and \mathbb{H} , respectively.

Lemma 1: Given $\alpha = \alpha_0 \in \mathbb{E}$, the function $\mathcal{G}(\alpha_0, \beta)$ is concave in β , given $\beta = \beta_0 \in \mathbb{H}$, the function $\mathcal{G}(\alpha, \beta_0)$ is concave in α ; Given $\alpha = \alpha_0 \in \mathbb{E}$, the function $\mathcal{H}(\alpha_0, \beta)$ is concave in β , given $\beta = \beta_0 \in \mathbb{H}$, the function $\mathcal{H}(\alpha, \beta_0)$ is concave in α .

Proof: The proof is provided in Appendix B.

Combining the Theorem 1 and Lemma 1, we can draw a conclusion that the optimization problem (P1) is biconcave for $\alpha \in \mathbb{E}$ and $\beta \in \mathbb{H}$, since (P1) is concave in β for given $\alpha = \alpha_0 \in \mathbb{E}$ and concave in α for given $\beta = \beta_0 \in \mathbb{H}$.

4.2 Algorithm for Solving Biconcave Problem

Based on the definitions of convex function and concave function, it is fact that if a function $f : B \rightarrow \mathbb{R}$ is biconvex, then the function $g : -f$ is biconcave on B [10]. From literature [10], an Alternate Convex Search (ACS) was proposed to solve the biconvex optimization problem, which is a minimization method and a special case of the Block-Relaxation Methods. Thus, we can utilize the core concept of the ACS to construct an algorithm for biconcave optimization problem. The specific procedure is illustrated in Algorithm 1.

Algorithm 1. Optimal algorithm for problem (P1)

Step 1: Choose an arbitrary starting point $z_0 = (\alpha_0, \beta_0) \in B$ and initialize $j = 0$, where $B = \mathbb{E} \times \mathbb{H}$ represents the biconcave set for α and β ;

Step 2: Solve the following concave optimization problem with fixed $\beta = \beta_j$

$$\begin{aligned} & \max \{ \mathcal{G}(\alpha, \beta_j), \alpha \in B_{\beta_j} \} \\ & \text{s.t. } \mathcal{H}(\alpha, \beta_j) \geq r_P, \alpha \in B_{\beta_j}. \end{aligned}$$

If we can obtain an optimal solution $\alpha^* \in B_{\beta_j}$, then set $\alpha^* = \alpha_{j+1}$; otherwise STOP;

Step 3: Solve the following concave optimization problem with fixed $\alpha = \alpha_{j+1}$

$$\begin{aligned} & \max \{ \mathcal{G}(\alpha_{j+1}, \beta), \beta \in B_{\alpha_{j+1}} \} \\ & \text{s.t. } \mathcal{H}(\alpha_{j+1}, \beta) \geq r_P, \beta \in B_{\alpha_{j+1}}. \end{aligned}$$

If an optimal solution $\beta \in B_{\alpha_{j+1}}$ can be obtained to this problem, then set $\beta^* = \beta_{j+1}$; otherwise STOP;

Step 4: If the result $z_{j+1} = (\alpha_{j+1}, \beta_{j+1})$ satisfies the predefined stopping criterion, then STOP; otherwise update $j = j+1$ and go back to **Step 2**.

5 Numerical and Simulation Results

In this section, we demonstrate the numerical results to verify the accuracy of the theoretical analyses in Sect. 3 with Monte Carlo simulations. We utilize the proposed algorithm in Sect. 4 to solve the optimization problem and obtain optimal coefficients α and β . Without otherwise specified, we set the system parameters as: the power of noise $\delta_0 = -30$ dBm, path loss exponent $\theta = 3$, the energy conversion efficiency $\eta = 0.5$, the distance $d_{PS} = 4$ m and $d_{SP} = (10 - d_{PS})$ m.

5.1 Outage Probability of Primary System

Figure 2 shows the outage probability of the primary system with regards to the primary transmission power P_P for different primary rates γ_P . The figure shows that the outage performance of the primary system gets better with the increase of the transmission power P_P . Moreover, the primary outage performance is deteriorated with the increase of γ_P from 0.55 bit/s/Hz to 1.15 bit/s/Hz since it is more difficult for channel to support a higher rate requirement. The analytical results of the primary outage probability agree well with the Monte-Carlo simulations, which verifies the analysis in Sect. 3.

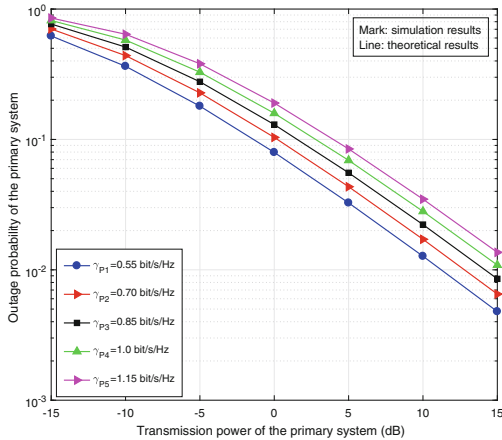


Fig. 2. The outage probability of the primary system with regards to the primary transmission power P_P for different primary rates γ_P .

Figure 3 shows the outage probability of the primary system with respect to transmission distance d_{PS} for different primary rates γ_P . From this figure, the primary outage performance deteriorates first and then improves with the increase of d_{PS} . When the transmission distance d_{PS} increases from 1 m to 5 m, the harvested RF energy at the ST becomes lower, which results in a less opportunity of spectrum access, so that the outage probability is increased. However,

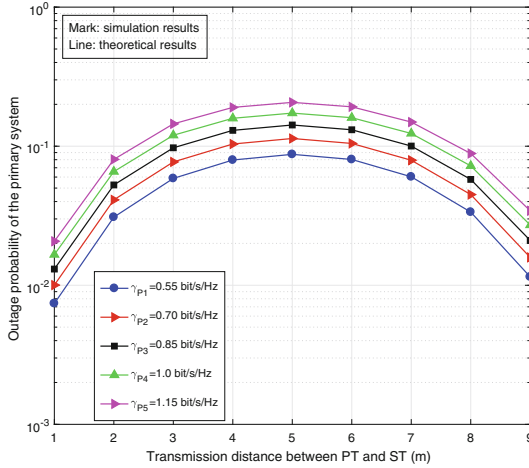


Fig. 3. the outage probability of the primary system with respect to transmission distance d_{PS} for different primary rates γ_P .

when d_{PS} increases from 5 m to 9 m, although the harvested energy continuous declination, the transmission distance between the ST and PR gets shorter, so the primary outage probability is decreased. Similar to the previous analysis, the lower primary transmission rate requirement will result in a better primary outage performance because the smaller the target rate, the higher the probability of the channel supporting the transmission. The analytical results also agree well with the simulation results.

5.2 Secrecy Outage Performance of Secondary System

Figure 4 shows the SOP of the secondary system with regards to the primary transmission power P_P for different secrecy capacity threshold C_{th} . We can see that the SOP of the secondary system is decreased with increase of transmission power P_P . The secondary SOP improves with the lower secrecy capacity threshold C_{th} because the secrecy capacity is easier to support a lower capacity threshold. As observed from this figure, the secondary SOP for large $\lambda_{SR}/\lambda_{SE}$ outperforms the one for small $\lambda_{SR}/\lambda_{SE}$ with fixed C_{th} and P_P , which means that the secondary system can achieve a higher transmission rate being listened by eavesdropper SE when channel quality between ST and SR is better than the link between ST and SE. The SOP of the secondary system analyzed in Sect. 3 is validated because the theoretical results coincide exactly with the simulation results.

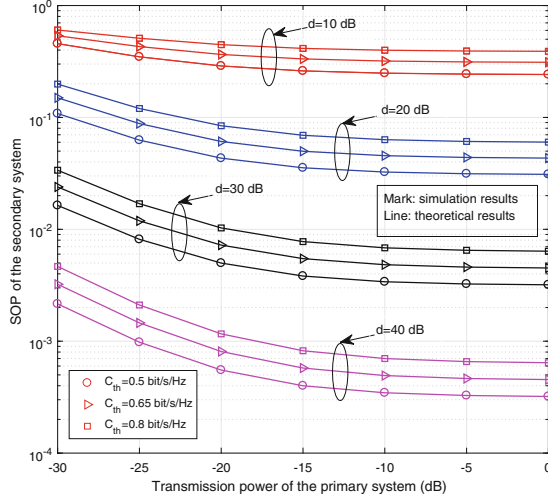


Fig. 4. The SOP of secondary system with regards to the primary transmission power P_P for different secrecy capacity threshold C_{th} . $d = \lambda_{SR}/\lambda_{SE}$

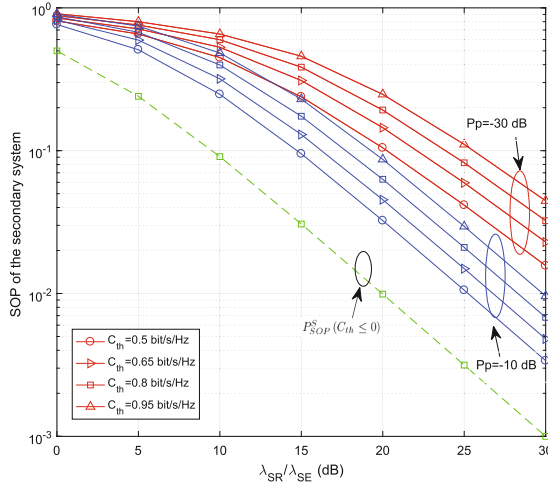


Fig. 5. The SOP of the secondary system with regards to the $\lambda_{SR}/\lambda_{SE}$.

Figure 5 illustrates the SOP of the secondary system with regards to the $\lambda_{SR}/\lambda_{SE}$ for different secrecy capacity threshold C_{th} . As depicted in Fig. 5, with the increase of $\lambda_{SR}/\lambda_{SE}$, i.e., the secondary secrecy capacity is improved, the secondary SOP is decreased since the ST-SR link is getting better than ST-SE link. Similar to the previous analysis, the higher secrecy capacity threshold will result in a lower SOP for the secondary system. Therefore, in this case, the lower the secrecy capacity threshold, the higher the secondary SOP. Based on (21),

we have $P_{SOP}^S(C_{th} \leq 0) = 1 - P_{PNSC}^S$, which denotes the SOP of the secondary system under the condition of zero secrecy capacity and it also can be used as the low-bound of the secondary SOP.

6 Conclusion

In this paper, we considered an overlay cognitive radio network with wireless-powered relay, then analyzed the primary outage probability and the secrecy outage probability and probability of non-zero secrecy capacity of the secondary system, which have been verified by simulations. Furthermore, we formulated an optimization problem to improve the system performance and proposed a jointly optimal algorithm to solve optimization problem through proving the biconvexity of optimization problem. We observed from the numerical results that our proposed transmission scheme can provide greater secure information transmission for secondary system and guarantee the outage performance for primary system.

A Proof of Proposition 1

Let $X = |h_{PS}|^2$ and $Y = |h_{SP}|^2$, we can define $W = \frac{lXY}{mY + \delta_{PR}}$, where the cumulative distribution function (c.d.f) of W is given by

$$F_W(w) = \Pr \left\{ \frac{lXY}{mY + \delta_{PR}} < w \right\} = \Pr \{ Y(lX - wm) < w\delta_{PR} \}. \quad (23)$$

Therefore, $F_W(w)$ can be further written as

$$\begin{aligned} F_W(w) &= \Pr \left\{ Y < \frac{w\delta_{PR}}{lX - wm} \mid X > \frac{wm}{l} \right\} \Pr \left\{ X > \frac{wm}{l} \right\} \\ &+ \Pr \left\{ Y \geq \frac{w\delta_{PR}}{lX - wm} \mid X \leq \frac{wm}{l} \right\} \Pr \left\{ X \leq \frac{wm}{l} \right\} \\ &= \Pr \left\{ Y < \frac{w\delta_{PR}}{lX - wm} \mid X > \frac{wm}{l} \right\} \Pr \left\{ X > \frac{wm}{l} \right\} + \Pr \left\{ X \leq \frac{wm}{l} \right\}, \end{aligned} \quad (24)$$

where

$$\begin{aligned} &\Pr \left\{ Y < \frac{w\delta_{PR}}{lX - wm} \mid X > \frac{wm}{l} \right\} \\ &= \int_{\frac{wm}{l}}^{\infty} \frac{1}{\lambda_{PS}} \exp\left(-\frac{x}{\lambda_{PS}}\right) - \frac{1}{\lambda_{PS}} \exp\left(-\frac{x}{\lambda_{PS}} - \frac{w\delta_{PR}}{\lambda_{SP}(lx - wm)}\right) dx. \end{aligned} \quad (25)$$

Defining a new integration variable $\bar{x} \triangleq x - wm/l$, the above Eq. (25) can be rewritten as

$$\begin{aligned} &\Pr \left\{ Y < \frac{w\delta_{PR}}{lX - wm} \mid X > \frac{wm}{l} \right\} \\ &= \underbrace{\exp\left(-\frac{wm}{l\lambda_{PS}}\right)}_{Q_1} - \underbrace{\frac{1}{\lambda_{PS}} \exp\left(-\frac{wm}{l\lambda_{PS}}\right) \sqrt{\frac{4w\delta_{PR}\lambda_{PS}}{l\lambda_{SP}}} \mathcal{K}_1 \left(\sqrt{\frac{4w\delta_{PR}}{l\lambda_{PS}\lambda_{SP}}} \right)}_{Q_2}. \end{aligned} \quad (26)$$

Besides, we have

$$\begin{aligned}\Pr\left\{X > \frac{wm}{l}\right\} &= \exp\left(-\frac{wm}{l\lambda_{PS}}\right) = Q_1, \\ \Pr\left\{X \leq \frac{wm}{l}\right\} &= 1 - \exp\left(-\frac{wm}{l\lambda_{PS}}\right) = 1 - Q_1.\end{aligned}\quad (27)$$

Therefore, the outage probability of the primary system can be derived as (12).

B Proof of Theorem 1

B.1 Convexity of objective function $\mathcal{G}(\alpha, \beta)$

Based on mentioned Lemma 1 in [10], we can learn that $\log_2(p(x))$ is a concave function if $p(x)$ is a positive concave function. Therefore, for the given $\alpha = \alpha_0$, we re-define the following function

$$\tilde{\mathcal{G}}(\alpha_0, \beta) = \frac{1 + r_{SR}(\alpha_0, \beta)}{1 + r_{SE}(\alpha_0, \beta)} = \frac{1 + \frac{\alpha_0\beta\eta P_P|h_{PS}|^2|h_{SR}|^2}{(1-\alpha_0)\delta_0}}{1 + \frac{\alpha_0\beta\eta P_P|h_{PS}|^2|h_{SE}|^2}{(1-\alpha_0)\delta_0}} \quad (28)$$

as auxiliary function to demonstrate the convexity of $\mathcal{G}(\alpha_0, \beta)$ through analyzing its secondary derivative with respect to β , which is given by

$$\frac{\partial^2 \tilde{\mathcal{G}}(\alpha_0, \beta)}{\partial \beta^2} = \frac{2\alpha_0^2(\alpha_0 - 1)\eta^2 P_P^2|h_{PS}|^4|h_{SE}|^2\left(|h_{SR}|^2 - |h_{SE}|^2\right)}{\alpha_0\eta P_P|h_{PS}|^2|h_{SE}|^2\beta + (1 - \alpha_0)\delta_0}. \quad (29)$$

Obviously, the $\tilde{\mathcal{G}}(\alpha_0, \beta) > 0$ and the $\tilde{\mathcal{G}}(\alpha_0, \beta)$ is concave in β since the value $\frac{\partial^2 \tilde{\mathcal{G}}(\alpha_0, \beta)}{\partial \beta^2}$ is always negative. Thus, we can proof that the $\mathcal{G}(\alpha_0, \beta)$ is also concave in β .

For the given $\beta = \beta_0$, the second partial derivative of $\mathcal{G}(\alpha, \beta_0)$ is given by

$$\frac{\partial^2 \mathcal{G}(\alpha, \beta_0)}{\partial \alpha^2} = \frac{\varpi - \pi}{2 \ln 2 [(\varpi - 1)\alpha + 1]^2} \times \frac{2\varpi\pi\alpha + (\varpi + \pi)(1 - \alpha)}{[(\pi - 1)\alpha + 1]^2}, \quad (30)$$

where

$$\varpi = \frac{\beta_0\eta P_P|h_{PS}|^2|h_{SE}|^2}{\delta_0}, \pi = \frac{\beta_0\eta P_P|h_{PS}|^2|h_{SR}|^2}{\delta_0}.$$

Based on aforementioned analysis, the value of $\frac{\partial^2 \mathcal{G}(\alpha, \beta_0)}{\partial \alpha^2}$ is clearly negative, which can certainly prove that the $\mathcal{G}(\alpha, \beta_0)$ is concave in α .

B.2 Convexity of Constraint Function $\mathcal{H}(\alpha, \beta)$

To simplify the proving process, we also assume $\delta_{ST} = \delta_{PR} = \delta_C = \delta_0$ in the followings. For the given $\alpha = \alpha_0$, the $\mathcal{H}(\alpha_0, \beta)$ is given by

$$\mathcal{H}(\alpha_0, \beta) = \frac{1 - \alpha_0}{2} \log_2 \left(1 + \frac{\frac{\alpha_0}{1 - \alpha_0} \beta \eta P_P |h_{PS}|^2 |h_{SP}|^2}{\left(\frac{\alpha_0}{1 - \alpha_0} \beta \eta \delta_0 + \frac{\alpha_0}{1 - \alpha_0} \frac{\beta}{1 - \beta} \eta \delta_0\right) |h_{SP}|^2 + \delta_0} \right). \quad (31)$$

Based on above-mentioned analyses, the convexity of $\mathcal{H}(\alpha_0, \beta)$ can be demonstrated through analyzing the convexity of $r_{PR}(\alpha_0, \beta)$ with respect to β . Thus, we have

$$\frac{\partial^2 r_{PR}(\alpha_0, \beta)}{\partial \beta^2} = - \frac{4\theta}{\varphi\beta^2(1-\beta)^2\left(\frac{1}{1-\beta} + \frac{1}{\varphi\beta} + 1\right)^3} \frac{2\left(1 + \frac{1}{\varphi\beta}\right)\theta}{2\left(1 + \frac{1}{1-\beta}\right)\theta} \quad (32)$$

$$- \frac{(1-\beta)^3\left(\frac{1}{1-\beta} + \frac{1}{\varphi\beta} + 1\right)^3}{\varphi\beta^3\left(\frac{1}{1-\beta} + \frac{1}{\varphi\beta} + 1\right)^3},$$

where $\theta = P_P|h_{PS}|^2/\delta_0$ and $\varphi = \alpha_0\eta|h_{PS}|^2/(1-\alpha_0)$. Though the analysis of the above-mentioned equation, the result of (32) is clearly positive real number. As a result, $\mathcal{H}(\alpha_0, \beta)$ is concave in β .

For the given $\beta = \beta_0$, it is difficult to derive the exact result of the second partial derivative of $\mathcal{H}(\alpha, \beta_0)$ with respect to α since its non-convexity, an approximate expression when the primary system operates at high SNR region is used to proof the convexity of $\mathcal{H}(\alpha, \beta_0)$ [10], which is given by

$$\mathcal{H}(\alpha, \beta_0) \approx \tilde{\mathcal{H}}(\alpha, \beta_0) = \frac{1-\alpha}{2} \log_2 \left(\frac{\varsigma\alpha}{(\lambda-1)\alpha+1} \right), \quad (33)$$

where

$$\varsigma = \frac{P_P\beta_0\eta|h_{PS}|^2|h_{SP}|^2}{\delta_0}, \lambda = \frac{(2-\beta_0)\beta_0\eta|h_{SP}|^2}{1-\beta_0}.$$

The corresponding second partial derivative of $\tilde{\mathcal{H}}(\alpha, \beta_0)$ with respect to α is then given by

$$\frac{\partial^2 \tilde{\mathcal{H}}(\alpha, \beta_0)}{\partial \alpha^2} = - \frac{2\lambda\alpha + 1 - \alpha}{2\ln^2\alpha^2[(\lambda-1)\alpha+1]^2}. \quad (34)$$

Obviously, it is easy to find that the $\tilde{\mathcal{H}}(\alpha, \beta_0)$ is concave in α .

References

1. Ullah, H., Nair, N.G., Moore, A., et al.: 5G communication: an overview of vehicle-to-everything, drones, and healthcare use-cases. *IEEE Access* **7**, 37251–37268 (2019)
2. Ji, P., Jia, J., Chen, J.: Joint optimization on both routing and resource allocation for millimeter wave cellular networks. *IEEE Access* **7**, 93631–93642 (2019)
3. Sharma, M., Sahoo, A.: Stochastic model based opportunistic channel access in dynamic spectrum access networks. *IEEE Trans. Mob. Comput.* **13**(7), 1625–1639 (2014)
4. Wang, C., Li, Y., Yang, Y., et al.: Combing solar energy harvesting with wireless charging for hybrid wireless sensor networks. *IEEE Trans. Mob. Comput.* **17**(3), 560–576 (2018)
5. Chen, H., Zhai, C., Li, Y., et al.: Cooperative strategies for wireless-powered communications: an overview. *IEEE Wirel. Commun.* **25**(4), 112–119 (2018)

6. Tang, K., Shi, R., Dong, J.: Throughput analysis of cognitive wireless acoustic sensor networks with energy harvesting. *Future Gener. Comput. Syst.* **86**, 1218–1227 (2018)
7. Jiang, L., Tian, H., Qin, C., et al.: Secure beamforming in wireless-powered cooperative cognitive radio networks. *IEEE Commun. Lett.* **20**(3), 522–525 (2016)
8. Zhang, J.-L., Pan, G.-F., Wang, H.-M.: On physical-layer security in underlay cognitive radio networks with full-duplex wireless-powered secondary system. *IEEE Access* **4**, 3887–3893 (2016)
9. Gradshteyn, I.-S., Ryzhik, I.-M.: *Table of Integrals, Series, and Products*, 7th edn. Academic Press, New York (2007)
10. Gorski, J., Puffer, F., Klamroth, K.: Biconvex sets and optimization with biconvex functions: a survey and extensions. *Math. Methods Oper. Res.* **66**(3), 373–407 (2007)